

NUMERICAL AND ANALYTICAL CALCULATIONS IN BALL BEARINGS

Luc Houpert

TIMKEN Research Europe
B.P. 89, 68002 Colmar, France
Tel.: +33 3 89 21 44 61 Fax: +33 3 89 21 45 92 Email: houpert@timken.com

ABSTRACT

Numerical calculations of the shaft and bearing misalignment, conducted with an in house developed code, are done to illustrate the influence of the housing described as a hollow shaft or more generally as a stiffness matrix obtained by Finite Element Analysis (F.E.A.). A full coupling between several outer races is therefore considered.

Analytical ball bearing torque calculations are also developed for deriving simple but powerful relationships giving the friction moments and the location of the pure rolling lines in the contact. The novelty of the study lies in the analytical relationships (as opposed to numerical) which enable the reader to design and optimize easily a bearing for a specific application. Furthermore, the location of the pure rolling lines has been derived without the zero net friction force assumption, which should allow the reader to better predict the bearing kinematics and hence ball – cage pocket clearance and better calculate the friction moments.

Useful curve-fitted relationships are also given for defining the Hertzian contact dimensions and pressure, and a methodology is given with appropriate relationships or references for defining the full bearing stiffness matrix, useful when calculating system resonance frequencies.

1 OBJECTIVES

Bearing torque, stiffness and life are important performance parameters that need to be known.

Most of the time, these performance parameters are calculated numerically using computer tools such as the one of Jones, (ref. 1) or Gupta (ref. 2) in which the outputs are calculated as a function of many input variables. An optimization of a bearing design can be obtained by scanning on the input variables and by performing a kind of numerical trial and error approach.

We did develop a general computer code which makes use of a non linear Finite Element Analysis (F.E.A.) and of the bearing, shaft and housing elasticity. The model has been described in ref. 3 to 5 by Houpert.

Using this code, we first would like to illustrate, by an example, the effect of the housing elasticity which is creating a coupling between the outer races. As a result,

the bearing loads and moments and deflections will be better described.

Instead of using numerical solutions, it is also interesting to develop simplified analytical models and to use analytical solutions (as opposed to numerical calculations) which are more convenient for designing a bearing and making an initial bearing selection.

Key input parameters are then easily identified which facilitates the compromise to find for obtaining in general low bearing torque, large bearing stiffness and an appropriate bearing life.

The objectives of this paper are to show such analytical models and demonstrate how they can be used for calculating bearing torque and for designing ball bearings in a general system.

2 NUMERICAL CALCULATION: EFFECT OF HOUSING

Figure 1 shows a simple (1 shaft + 2 bearings) application in which the load is applied in the middle of the shaft and the housing has the shape of a hollow tube. Two shafts can therefore be used: one shaft (shaft 1) connecting the inner races, and another one (shaft 2) representing the housing and connecting the outer races. Let's assume that the shaft 2 is fixed by a infinitely rigid spring at one end.

As explained in ref. 3 to 5, the non linear F.E.A. approach consists of calculating the five displacements (3 translations and two rotations) at all nodes.

Figure 2 shows the calculated deflected shafts and corresponding relative bearing misalignment. Deformations have been magnified 50 times and initial position is shown as dotted line.

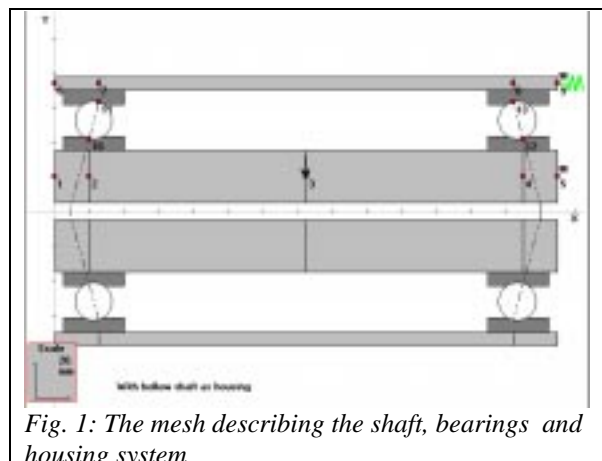


Fig. 1: The mesh describing the shaft, bearings and housing system

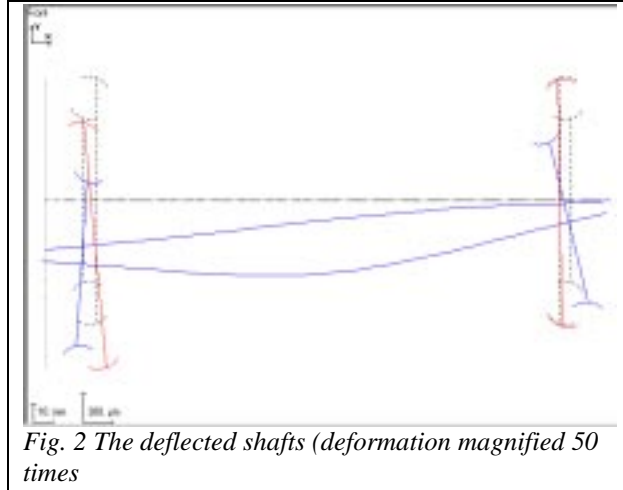


Fig. 2 The deflected shafts (deformation magnified 50 times)

The shaft deflection is not symmetrical and the bearing misalignment is equal to 3.17 and 4.42 mrad in the two bearings.

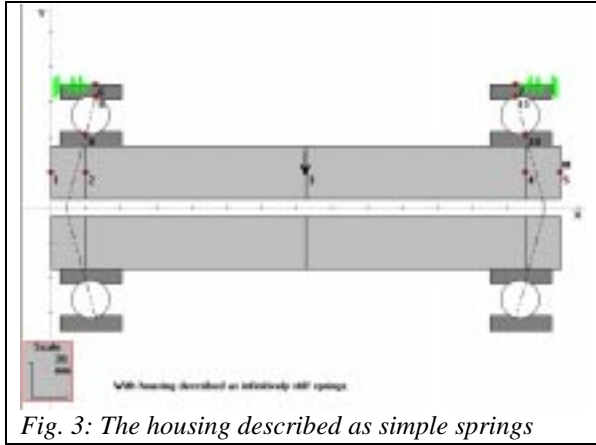


Fig. 3: The housing described as simple springs

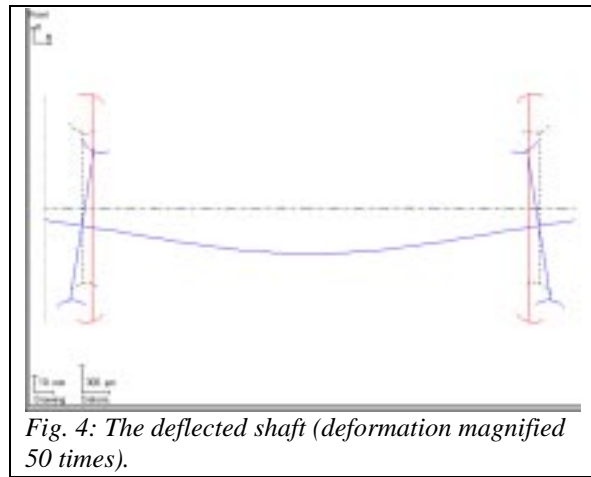


Fig. 4: The deflected shaft (deformation magnified 50 times).

Classical bearing computer codes making use of the shaft bending would usually consider the first shaft only, but describe the housing as simple independent springs, chosen infinitively rigid when stiffness values are not known as shown on Figure 3. The corresponding

calculated shaft deflection and relative bearing misalignment is shown on Figure 4.

The shaft deflection is now symmetrical and the bearing misalignment is 3.14 mrad in both bearing (instead of 3.17 and 4.42 mrad. in the previous simulation).

Noticeable bearing performance differences can therefore be calculated as a function of how the housing is described, which is the point of our demonstration.

3 ANALYTICAL BEARING TORQUE CALCULATION.

The following is an extension of the initial work of Snare (ref. 6).

Fig. 5 shows a ball between the two races. The contact angles on both races are identical in this Figure, but the general case where they differ because of centrifugal effects is considered in this paper. We will assume outer race control, i.e. the ball rotational vector ω_r is parallel to the outer race contact tangent.

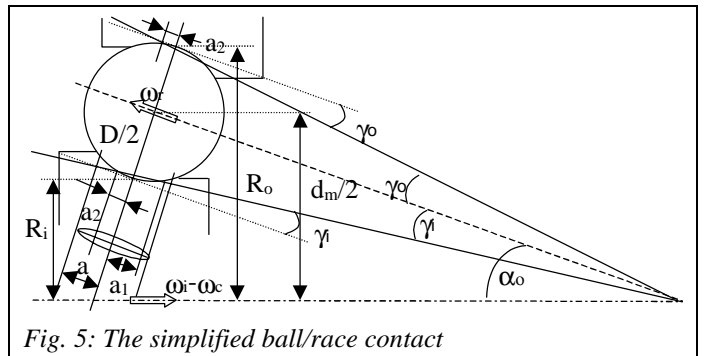


Fig. 5: The simplified ball/race contact

It can then be demonstrated on the outer race (OR) that:

$$\text{tg} \gamma_o \approx \frac{D \cdot \sin \alpha_o}{d_m}$$

where γ_o , D , α_o and d_m are defined in Figure 5.

Calculations are more complex on the inner race (IR) when $\alpha_o \neq \alpha_i$. It can be demonstrated that :

$$\gamma_i \approx -\arcsin \left\{ \frac{2 \cdot R_i \cdot \sin \alpha_o}{\sqrt{D^2 \cdot \sin^2 \alpha_o + d_m^2 - 2 \cdot D \cdot d_m \cdot \sin(\alpha_o - \alpha_i) \cdot \sin \alpha_o}} \right\} + \alpha_i$$

It is also demonstrated in the appendix that the locations a_1 ($a_1 < 0$) and a_2 ($a_2 > 0$) of the pure rolling lines is only function of the parameter E defined by:

$$E = \frac{2 \cdot R_a}{a} \cdot \text{tg} \gamma \approx \frac{2 \cdot R_a}{a} \cdot \frac{D \cdot \sin \alpha}{d_m} \quad (\text{on OR})$$

with R_a being the Hertzian contact radius:

$$R_a = \frac{D}{2} \cdot \frac{1+K}{1+K/2} \approx \frac{D}{2} \left(1 + \frac{K}{2} \right)$$

a being the semi ellipse length (defined later) and K the parameter describing the radius of curvature of the race,

i.e. the race curvature radius is $(1+K)/\frac{D}{2}$.

We show in the appendix that the location a_1 and a_2 of the pure rolling lines are coupled by the following relationship :

$$\frac{a_1}{a} = -\left(\frac{a_2}{a} + E\right)$$

Figure 6 shows more precisely the sliding speed distribution on the elliptical contact as well as two friction moments, MC and MP that we will calculate later.

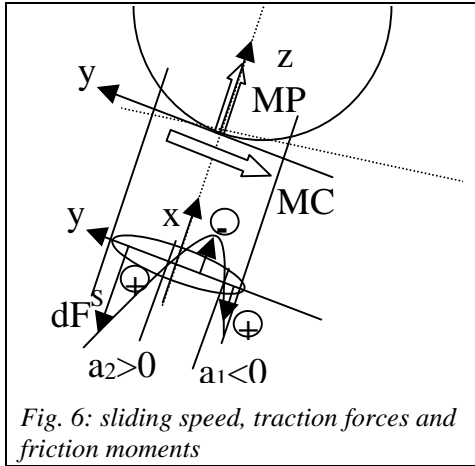


Fig. 6: sliding speed, traction forces and friction moments

The sliding speed (race speed – ball speed) is due to the curved ellipse in space and can be positive or negative depending on the ellipse slice considered. This sliding speed is responsible of a friction shear stress τ calculated as :

$$\tau = \pm \mu . P$$

where P is the local Hertzian pressure and μ the local friction coefficient that we will discuss later.

The integral of the shear stress along a given slice gives the elementary positive or negative sliding traction force dF^S defined by (see appendix):

$$dF^S = \int_{-b_1}^{b_1} \tau . dx = \pm \frac{3}{4} . \mu . Q . (1 - Y^2) dY \quad \text{with } Y = \frac{y}{a}$$

The integral of the latter force along the entire ellipse (with dF^S negative for $a_1/a < Y < a_2/a$ and positive elsewhere) gives the final friction force F^S . In the appendix we show finally that:

$$F^S = \mu . Q . \left[1 - \frac{3}{2} . (2.Y_2 + E) + \frac{1}{2} . (Y_2^3 + (Y_2 + E)^3) \right] \quad \text{with } Y_2 = \frac{a_2}{a}$$

At this stage, we still don't know Y_2 but we will use the fact that all forces and moments applied on the ball, and listed on Figure 7, have to be in equilibrium, as explained in ref. 7 by Houpert.

FR are hydrodynamic rolling forces, FP are pressure forces, FB can be an additional braking force due to the cage or to inertial effects, MC is the curvature friction moment, MB an eventual additional braking moment and MER the elastic rolling resistance moment that we will describe later too.

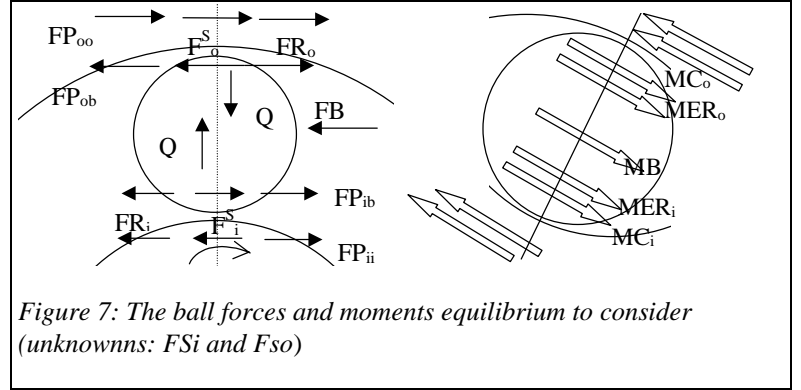


Figure 7: The ball forces and moments equilibrium to consider (unknowns: F^S_i and F^S_o)

We can take as unknowns the friction forces F^S_i and F^S_o on the two contacts and use the force and moments equilibrium to calculate F^S_i and F^S_o . Calculations can be conducted in the general case ($\alpha_o \neq \alpha_i$), but we will assume in the following $\alpha_o \approx \alpha_i$ to push as far as possible the analytical calculation and obtain simple ball bearing torque relationships.

It can then be shown that:

$$F_i^S = \frac{MC_o + MC_i + MER_i + MER_o + MB}{D} + FR_o + \frac{(FR_i + FR_o) . D . \cos \alpha}{d_m} + \frac{FB}{2}$$

$$F_o^S = \frac{MC_o + MC_i + MER_i + MER_o + MB}{D} + FR_i - \frac{(FR_i + FR_o) . D . \cos \alpha}{d_m} - \frac{FB}{2}$$

We see that F^S is usually small compare to $\mu . Q$ which justifies why Snare assumed it nil.

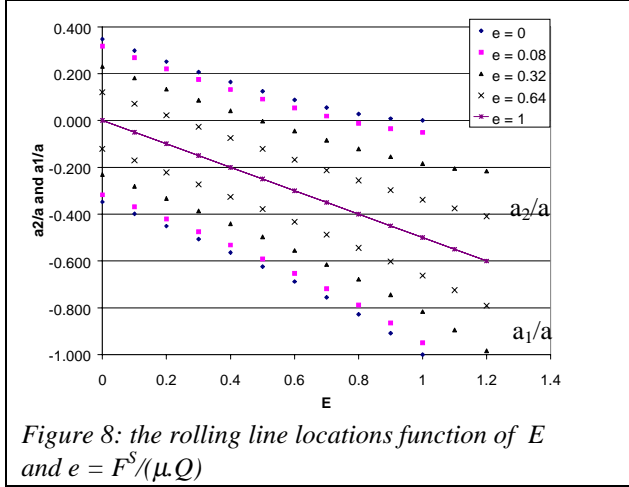
But there are circumstances (low load on inner race, large load on outer race because of centrifugal effects, large braking effects due to the cage) where F^S_i for example can be large. The main novelty in the following is that we will not fix F^S to zero.

Knowing F^S and its relationship versus Y_2 , we can now solve the following relationship in order to obtain the rolling line location Y_2 (or a_2/a) on both races:

$$\mu . Q . \left[1 - \frac{3}{2} . (2.Y_2 + E) + \frac{1}{2} . (Y_2^3 + (Y_2 + E)^3) \right] - F^S = 0 \quad \text{or}$$

$$1 - \frac{3}{2} . (2.Y_2 + E) + \frac{1}{2} . (Y_2^3 + (Y_2 + E)^3) - e = 0 \quad \text{with } e = \frac{F^S}{\mu . Q}$$

The general calculation of the rolling line location a_2/a versus E and e is also developed in the appendix and an analytical solution is obtained. Results are shown versus E on Figure 8 for several values of e (hence F^S).



For E and e nil, the two rolling line are symmetrical and equal to ± 0.347 . For E larger than 1 and e small, only one rolling line is found, $a_2/a = 0$, the other one (a_1/a) being out of the contact ellipse.

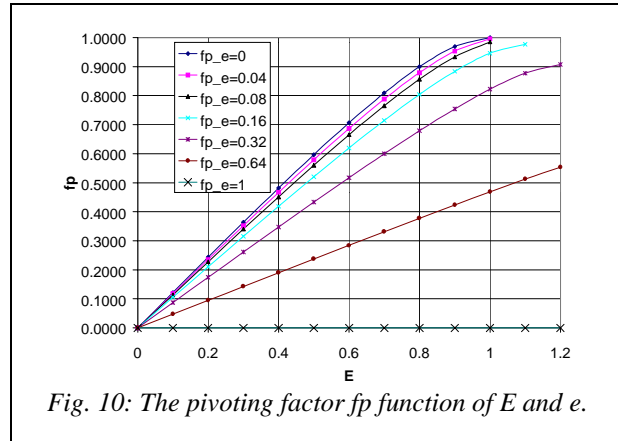
When F^S is not nil and gets large, the two rolling lines (a_2/a and a_1/a) get closer and can be both on the negative side of the y axis and even coincide as one single line when $e = 1$, i.e. for the maximum value of F^S .

The knowledge of the two rolling lines on the inner and outer race contacts is important because it enables us to calculate precisely the roller rotational speed ω_r and orbital speed ω_c which can be used for calculating the relative displacement during one cage revolution of the ball in its pocket and hence the appropriate ball – cage pocket clearance.

We can now define the friction moment MC and MP . The shape of the contact ellipse in space can be approximated as a parabola and used for calculating the friction moments MC and MP .

$$z \approx \frac{y^2}{2.R_a} \quad MC = \int_{-a}^{+a} dF^S . z \quad MP = \int_{-a}^{+a} dF^S . y$$

MC is defined as the friction moment due to the curvature shape of the ellipse while MP is the friction moment due to pivoting effects. The calculation of these two friction moments is developed in the appendix with



the assumption that the friction coefficient is constant over the contact ellipse.

When two rolling lines are found on the contact, MC and MP can be written:

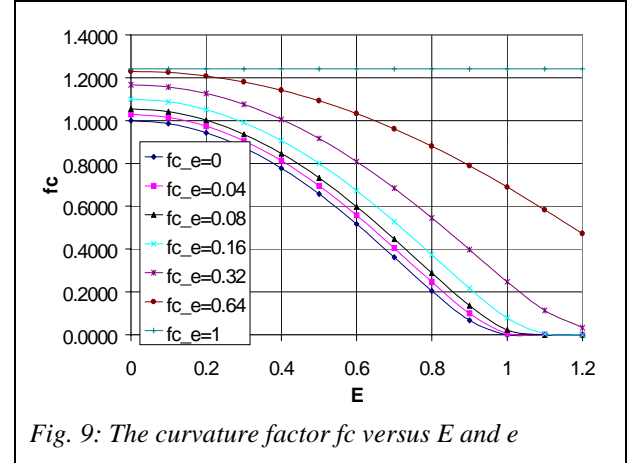
$$MC = 0.1\mu.Q.\frac{a^2}{R_a} \left\{ 1 - \frac{5}{2} (Y_2^3 - Y_1^3) + \frac{3}{2} (Y_2^5 - Y_1^5) \right\}$$

$$= 0.0806 \mu.Q.\frac{a^2}{R_a} . fc$$

$$MP = \frac{3}{8} . \mu.Q.a. \left\{ 2. [Y_1^2 - Y_2^2] - [Y_1^4 - Y_2^4] \right\}$$

$$= \frac{3}{8} . \mu.Q.a. fp$$

where fc and fp are the curvature and pivoting factors only function of E and e and shown on Figure 9 and 10.



We see that these two factors are competing. As E increases, fc decreases and fp increases.

As F^S gets larger, fc increases substantially and fp decreases, to zero when e equals 1 because the sliding forces dF^S are then all pointing in the same direction.

A curve-fitting can also be suggested when the assumption F^S or e equal zero is used and $E < 1$:

$$fc \approx 1.0026 - 0.1653 E - 0.2638 E^2 - 2.5521 E^3 + 1.9749 E^4$$

$$fp \approx 0.0042 + 1.1045 E + 0.4625 E^2 - 0.5648 E^3$$

For E larger than 1, fc is nil and fp is fixed to 1.

We finally have to explain how to calculate the friction coefficient μ .

Complex calculations of the friction coefficient μ can be conducted as shown in ref. 7 to 10 by Houpert.

The lubricant rheological model is non linear viscous – elastic, or viscous – elastic plastic. The shear stress is a function of the shear rate (sliding speed divided by the lubricant film thickness), viscosity, limiting shear stress and lubricant elastic shear modulus.

The lubricant inlet shear heating as well as the temperature increase in the lubricant film need also to be calculated. The local lubricant traction coefficient varies then from slice to slice as a function of the pressure and sliding speed distribution. It is nil or small at or near the rolling lines and reach maximum values between 0.02 (for synthetic lubricant) to 0.10 (for high traction drive oils), a typical value being 0.05 for a mineral lubricant.

At low film thickness values (lower than the composite surface roughness), roughness effects need also to be considered and are responsible of an overall increase of the friction coefficient, of the order of 0.10 for a mineral lubricant (see ref. 9).

In order to simplify the study, a constant friction coefficient will be used. The latter can be calculated using the average sliding speed and average pressure for example.

Sliding speed can be calculated using the ball speed ω_r and ω_e , defined by the knowledge of the rolling line locations, and a simple non linear visco - elastic model gives the appropriate friction coefficient as a function of the average viscosity and shear rate (see ref. 10). Asperity effects can also be considered as shown in ref. 9.

Knowing the sliding forces, MC and MP and all other forces and moments on the ball and races (action - reaction), the final bearing torque can now easily be calculated on the two races.

On the inner race for example, the torque dT due to one ball is:

$$dT = 2.(FR_o + FR_i) \cdot \frac{R_o \cdot R_i}{d_m} + \frac{MC_i \cdot R_o + MC_o \cdot R_i}{D} + \frac{MER_i \cdot R_o + MER_o \cdot R_i}{D} + \frac{MP_i + MP_o}{2} \cdot \sin \alpha + \left(\frac{MB}{D} + \frac{FB}{2} \right) R_i$$

$$dT = dTR + dTC + dTER + dTP + dTB$$

where dTR, dTC, dTER, dTP and dTB are the individual one ball contribution on the torque of the hydrodynamic rolling resistance, curvature effects, elastic rolling resistance, pivoting effects and additional braking effects respectively.

The final torque is obtained by summation of the individual contribution dT of each ball.

4 ADDITIONAL USEFUL ANALYTICAL OR CURVE-FITTED RELATIONSHIPS

Following are some useful relationships needed for conducting the calculations optimizing a design.

The maximum load Q_{max} and load distribution $Q(\psi)$ is needed and has been described in ref. 11 by Houpert. If F_r and F_a are the radial and axial bearing load, Z the number of balls, then:

$$Q_{max} = \frac{F_r}{Z \cdot J_r \cdot \cos \alpha} = \frac{F_a}{Z \cdot J_a \cdot \sin \alpha}$$

$$Q = Q_{max} \cdot \left(1 - \frac{1}{2 \cdot \epsilon} \cdot (1 - \cos \psi) \right)^{1.5}$$

where J_r and J_a are the classical Sjövall integrals and ϵ the load zone parameter function of $F_r \cdot \tan \alpha / F_a$.

Two typical cases are the pure thrust load, where $J_a = 1$ and ϵ is infinite (all balls are then loaded equally) and the case where half of the balls are loaded with $\epsilon = 0.5$ and $J_r = 0.2288$ because two bearings are mounted in opposite direction and the relative axial inner - outer race displacement is nil.

Knowing the load, we can now calculate the ellipse dimension a and other Hertzian related parameters. We first need to define the equivalent contact radius R_x on the inner and outer race and the ratio k of the equivalent radii (R_y/R_x).

$$R_{xi} = \frac{D}{2} \cdot \left(1 - \frac{D \cdot \cos \alpha}{d_m} \right) \quad R_{xo} = \frac{D}{2} \cdot \left(1 + \frac{D \cdot \cos \alpha}{d_m} \right)$$

$$k_i = \frac{1 + K_i}{K_i} \cdot \frac{1}{1 - \frac{D \cdot \cos \alpha}{d_m}} \quad k_o = \frac{1 + K_o}{K_o} \cdot \frac{1}{1 + \frac{D \cdot \cos \alpha}{d_m}}$$

General curve-fitted relationships for calculating the ellipse dimensions a and b as well as the maximum Hertzian pressure P_H are given next:

$$\frac{a}{R_x} \approx 1.1552k^{0.4676} \left(\frac{Q}{E' \cdot R_x^2} \right)^{\frac{1}{3}} \quad \frac{b}{R_x} \approx 1.1502k^{-0.1876} \left(\frac{Q}{E' \cdot R_x^2} \right)^{\frac{1}{3}}$$

$$\frac{P_H}{E'} \approx 0.3593k^{-0.2799} \left(\frac{Q}{E' \cdot R_x^2} \right)^{\frac{1}{3}}$$

where E' is the equivalent Young's modulus equal to 2.2610^{11} Pa.

Using the previous relationships, it becomes easy to follow the effect of the curvature parameter K, or contact angle α on the Hertzian pressure (that should not exceed 4 GPa.) or ellipse dimension (avoid truncation).

Furthermore, we can now calculate the parameter E, MC, MP, dTC and dTP and minimize the bearing torque. MC varies for example as $Q^{1.66}$ and MP varies as $Q^{1.33}$ and are very sensitive to the parameter K affecting the ellipse dimension a.

Compromises will necessarily have to be found. A low torque is for example found with a small value of a, hence a large value of the curvature parameter K, which is then responsible of a large Hertzian pressure hence low bearing life.

The initial contact angle has also to be optimized. A large contact angle makes dTC nil, but dTP maximum, while the reverse is obtained with a zero contact angle. The contact angle affects also the load Q_{max} so that an optimum contact angle has to be defined too.

For the sake of completeness, we also repeat how the hydrodynamic rolling force and the elastic rolling moment MER, given in ref. 7, are calculated.

In ref. 7 we give FR and MER (using I.S. units) as:

$$FR = 2.86 E' R_x^2 k^{0.348} (\alpha' E')^{0.022} \left(\frac{\eta_0 u}{E' R_x} \right)^{0.66} \left(\frac{Q}{E' R_x^2} \right)^{0.47}$$

$$MER = 7.4810^{-7} \left(\frac{D}{2} \right)^{0.33} Q^{1.33} \left\{ -3.519 \cdot 10^{-3} (k-1)^{0.8063} \right\}$$

where α' is the pressure – viscosity parameter, η_0 is the initial dynamic viscosity and u the entrainment speed ($\omega_r D/2$).

The torque dTR and dTER can now be calculated as well as the effects of curvature or contact angle, or load zone.

Note that the latter relationship is not too different from Todd's proposal (ref. 12) in which an elastic rolling force is used, which can also be interpreted as an elastic moment by writing:

$$F_{Todd} = 0.00423 Q \frac{b}{D} \Leftrightarrow$$

$$MER_{Todd} = 0.0021 Q b \approx 3.96 \cdot 10^{-7} \left(\frac{D}{2} \right)^{0.33} k^{-0.1886} Q^{1.33}$$

Todd's elastic rolling resistance (also called hysteresis loss) is about 3 times smaller than Snare's one but the contribution of dTER is usually very small.

We also give in ref. 11 useful curve-fitted relationships for calculating the local Hertzian contact stiffness and final bearing force versus displacements. I.S. units are used again:

$$Q = 3.37 \cdot 10^7 \left(\frac{1 + \bar{K}}{\bar{K}} \right)^{0.345} \sqrt{D} \delta^{1.5}$$

where \bar{K} is the average race curvature parameter.

The load versus displacements relationships can be derived analytically for obtaining the bearing axial, radial and tilting stiffness, as well as all coupling stiffness terms (obtained by deriving for example the radial load versus the axial or angular displacements).

A full bearing stiffness matrix can then be defined and used for predicting resonance frequencies of the system.

CONCLUSIONS

We did show in this paper using a numerical example and an in house developed code how the housing elasticity can affect the bearing and shaft deflection, hence bearing misalignment and performance.

The full ball bearing torque theory has then been outlined, with an emphasis put on the analytical developments that provide simple relationships and allow easy bearing design optimization.

Although calculations are analytical, some novelties are included in the suggested new model, such as the calculation of the location of the rolling lines on the contact ellipse with the sliding traction force taken as

not nil. This is important for calculating correctly the friction moments MC and MP, as well as the bearing kinematics used for defining the required ball – cage pocket clearance.

The competition between the curvature effects and pivoting effects is outlined and the final torque can be calculated analytically as a function of key input parameters such as the initial contact angle, the race curvature parameters or the number of rolling elements. Useful curve-fitted relationships for calculating simply the Hertzian contact dimensions and contact pressure are also given, and a methodology, curve-fitted relationships and references for calculating the bearing stiffness are finally offered.

ACKNOWLEDGEMENT

The author would like to thank the TIMKEN Company for permission to publish this paper as well as his colleagues from TIMKEN Aerospace & Super Precision Bearings (formally known as MPB) for their interest shown in this work.

APPENDIX

Calculation of a_1/a versus a_2/a

a_2/a will be calculated later and assumed known in this chapter.

Using the symbols defined in figure 5 and 6, the heights z_1 and z_2 are defined by:

$$z_1 = \frac{a_1^2}{2.R_a} \quad z_2 = \frac{a_2^2}{2.R_a}$$

From the definition of the γ angle and using algebraic values for $a_2 (>0)$ and $a_1 (<0)$, we have:

$$a_2 - a_1 = \frac{z_1 - z_2}{tg \gamma} = \frac{1}{2.R_a \cdot tg \gamma} (a_1^2 - a_2^2)$$

$$= \frac{1}{2.R_a \cdot tg \gamma} (a_1 - a_2)(a_1 + a_2)$$

$$\text{or: } \frac{a_1}{a} = -\frac{a_2}{a} - \frac{2.R_a}{a} \cdot tg \gamma = -\left(\frac{a_2}{a} + E \right)$$

Calculation of the traction force in a given slice:

The local pressure reads:

$$P_H \cdot \sqrt{1 - \left(\frac{x}{b} \right)^2 - \left(\frac{y}{a} \right)^2}$$

On a slice located at y , the pressure reads:

$$P = P_H \cdot \sqrt{1 - \left(\frac{x}{b} \right)^2 - \left(\frac{y}{a} \right)^2} = P_H \cdot \sqrt{1 - \left(\frac{y}{a} \right)^2} \cdot \sqrt{1 - \left(\frac{x}{b_1} \right)^2}$$

$$P = P_{H1} \cdot \sqrt{1 - \left(\frac{x}{b_1} \right)^2} \quad \text{with } P_{H1} = P_H \cdot \sqrt{1 - \left(\frac{y}{a} \right)^2}$$

and with b_1 defined as the half slice length:

$$b_1 = b \sqrt{1 - \left(\frac{y}{a}\right)^2}$$

The friction force on this slice is finally (with $X = x/b_1$ and $Y = y/a$):

$$\begin{aligned} dF^S &= \int_{-b_1}^{b_1} \tau \cdot dx = \pm 2 \cdot \mu \cdot P_{H1} \left\{ \int_0^{b_1} \sqrt{1 - \left(\frac{x}{b_1}\right)^2} \cdot dx \right\} \cdot dy \\ &= \pm 2 \cdot b_1 \cdot \mu \cdot P_{H1} \cdot \left\{ \int_0^1 \sqrt{1 - (X)^2} \cdot dX \right\} \cdot dy \end{aligned}$$

$$\begin{aligned} dF^S &= \pm 2 \cdot b_1 \cdot \mu \cdot P_{H1} \cdot \frac{\pi}{4} \cdot dy \\ &= \pm 2 \cdot b \cdot \sqrt{1 - \left(\frac{y}{a}\right)^2} \cdot P_H \cdot \sqrt{1 - \left(\frac{y}{a}\right)^2} \cdot \frac{\pi}{4} \cdot a \cdot dY \\ dF^S &= \pm \frac{3}{4} \cdot \mu \cdot \frac{P_H}{1.5} \cdot \pi \cdot a \cdot b \cdot (1 - Y^2) dY = \pm \frac{3}{4} \cdot \mu \cdot Q \cdot (1 - Y^2) dY \end{aligned}$$

Calculation of the final traction force by performing the proper integration

Using now the appropriate sign for the friction force (i.e. negative for $Y_1 < Y < Y_2$ and positive elsewhere), the final friction force is obtained by integrating dF^S versus Y , Y ranging from -1 to 1 .

$$\begin{aligned} F^S &= \frac{3}{4} \cdot \mu \cdot Q \cdot \left\{ \int_{-1}^1 (1 - Y^2) dY - 2 \cdot \int_{Y_1}^{Y_2} (1 - Y^2) dY \right\} \\ &= \frac{3}{4} \cdot \mu \cdot Q \cdot \left\{ \frac{4}{3} - 2 \cdot \left(Y_2 - \frac{Y_2^3}{3} + (Y_2 + E) - \frac{(Y_2 + E)^3}{3} \right) \right\} \\ &= \mu \cdot Q \cdot \left[1 - \frac{3}{2} \cdot (2 \cdot Y_2 + E) + \frac{1}{2} \cdot (Y_2^3 + (Y_2 + E)^3) \right] \end{aligned}$$

Calculation of the final traction force from force and moment equilibrium:

We did show in the core of this paper that the sliding force F^S on both races can be calculated versus all other known forces and moments using the ball force and moment equilibrium.

Calculation of the rolling line location $Y_2 = a_2/a$

Knowing now F^S , it is possible to calculate Y_2 . Y_2 is obtained by solving the following equation of degree 3:

$$F^S = \mu \cdot Q \cdot \left[1 - \frac{3}{2} \cdot (2 \cdot Y_2 + E) + \frac{1}{2} \cdot (Y_2^3 + (Y_2 + E)^3) \right] = \varepsilon$$

Snare took the value ε as nil while we will solve the previous equation with respect to E and the parameter e defined as :

$$e = \frac{F^S}{\mu \cdot Q} = \frac{\varepsilon}{\mu \cdot Q}$$

By writing $x = Y_2 = a_2/a$, the general polynomial equation to solve is:

$$(1 - e) + \frac{1}{2} \cdot \left\{ x^3 + (x + E)^3 \right\} - \frac{3}{2} \cdot \{ 2 \cdot x + E \} = 0$$

3 real solutions are found, and we will keep the value smaller than 1 to obtain:

$$\frac{a_2}{a} = -\frac{E}{2} + 2 \cdot \sqrt{\frac{E^2}{4} - 1} \cdot \cos \left[\frac{\pi + \varphi}{3} \right]$$

$$\text{with } \cos \varphi = 0.5(1 - e) \cdot \left(\frac{E^2}{4} - 1 \right)^{-\frac{3}{2}}$$

$$\text{We also remind that: } \frac{a_1}{a} = -\left(\frac{a_2}{a} + E \right)$$

Figure 8 shows how a_2/a varies as a function of E and e . We see that a_2/a decreases versus E and e and can be negative when e (sliding force) is large and E too.

In this later case, the two rolling lines (a_2/a and a_1/a) are on the negative side of the y axis

As F^S gets larger, the two rolling lines gets closer and coincide when $e = 1$, i.e. $F^S = \mu \cdot Q$.

Positive slip is then obtained all over the contact ellipse.

Calculation of MC and MP:

The curvature moment dMC due to one slice is negative between Y_1 and Y_2 and positive elsewhere.

$$dMC = \pm \frac{3}{4} \cdot \mu \cdot Q \cdot (1 - Y^2) \cdot \frac{a^2}{2 \cdot R_a} \cdot Y^2 \cdot dY$$

By assuming μ constant over the contact ellipse (by taking in fact its average or a typical value), the friction coefficient can be taken out of the integral to write:

$$\begin{aligned} MC &= \frac{3}{4} \cdot \mu \cdot Q \cdot \frac{a^2}{2 \cdot R_a} \cdot \left\{ \int_{-1}^1 (Y^2 - Y^4) dY - 2 \cdot \int_{Y_1}^{Y_2} (Y^2 - Y^4) dY \right\} \\ &= 0.1 \mu \cdot Q \cdot \frac{a^2}{R_a} \cdot \left[1 - \frac{5}{2} \cdot (Y_2^3 + (Y_2 + E)^3) + \frac{3}{2} \cdot (Y_2^5 + (Y_2 + E)^5) \right] \end{aligned}$$

When only one rolling line is found (because $Y_1 < -1$)

then MC is calculated as:

$$MC = \left\{ \int_{-1}^1 dMC - 2 \cdot \int_{-1}^{Y_2} dMC \right\} = 0.1 \mu \cdot Q \cdot \frac{a^2}{R_a} \cdot \left[-\frac{5}{2} \cdot Y_2^3 + \frac{3}{2} \cdot Y_2^5 \right]$$

with Y_2 often nil leading to a MC value nil.

Similarly, with the existence of two rolling lines, MP is calculated as:

$$\begin{aligned} MP &= \frac{3}{4} \cdot \mu \cdot Q \cdot a \cdot \left\{ \int_{-1}^1 (Y - Y^3) dY - 2 \cdot \int_{Y_1}^{Y_2} (Y - Y^3) dY \right\} \\ &= \frac{3}{8} \cdot \mu \cdot Q \cdot a \cdot \left[2 \cdot (Y_2 + E)^2 - Y_2^2 \right] - \left[(Y_2 + E)^4 - Y_2^4 \right] \end{aligned}$$

while with one rolling line we obtain:

$$MP = \frac{3}{8} \cdot \mu \cdot Q \cdot a \cdot \left[1 - Y_2^2 \right]^2$$

i.e. MP is maximum if Y_2 equal zero.

For $e = 1$, ($F^S = \mu \cdot Q$), MC is maximum, MP is nil and the final torque is large because of the large F^S value applied on the races. In this latter case, the use of a proper non linear viscous model will then show that, the required sliding speed needed to obtain a large friction force is very large, especially when loads are small. This large sliding speed is obtained with a substantial reduction of the ball orbital speed, known as skidding.

REFERENCES

1. A.B.Jones, 'The A.B. Jones high speed ball and roller bearing analysis program' Jones Engineering Company.
2. P.K Gupta, 'Advanced Dynamics of Rolling Elements' Springer-Verlag New York Inc., 1984
3. L. Houpert, 'Prediction of bearing, gear and housing performances', presented at the «Rolling bearing Practice Today Seminar», London, February 1995. Proceeding of the I. Mech. E.
4. L. Houpert, 'Numerical simulation of bearing, gear and housing performances », presented at the S.I.A. Symposium, « Allégement du Véhicule », Paris, March 1997. Proceeding of the S.I.A. symposium.
5. L. Houpert, J. Merckling, «A succesful transition from physically measured to numerically simulated bearings, shafts, gears and housing deflections in a transmission », presented at the GPC'98 Global PowerTrain Congress, Detroit 1998. 'New Powertrain Material & Processes' Proceeding, p131-137.
6. B. Snare, 'Rolling resistance in loaded ball bearing', Ball Bearing Journal n° 158, 1968
7. L. Houpert, P. Leenders, «A theoretical and experimental investigation into Rolling Bearing friction», presented at the 1985 Eurotrib Conf., Lyon ; Proc. Eurotrib Conf., 1985
8. L. Houpert, L. Flamand, D. Berthe, 'Rheological and thermal effects in a lubricated EHD contact' . ASME Journ. Lubr. Techn., Vol. 103, p. 526-533, 1981
9. L. Houpert, P. Leenders, «A study of mixed lubrication in modern Deep Groove Ball Bearings», presented at the 11th Leeds-Lyon Symp., Leeds ; Proc. 11th Leeds-Lyon Symp., 1984
10. L. Houpert, 'Fast calculations of EHD sliding traction forces; application to rolling bearings', presented at the 1984 ASLE / ASME Lubr. Conf., San Diego ; ASME Jour. Trib., Vol. 107, p. 234-240, 1985
11. L. Houpert, 'A Uniform analytical approach for ball and roller bearing', presented at the STLE-ASME Tribology Conf., (poster session), San Francisco, 1996. ASME Jour. Trib., Vol. 119, p. 851 - 857, oct. 1997.
12. M.J Todd and K.T. Stevens, 'Frictional torque of angular contact ball bearings with different conformities', ESA TRIB/1 paper, 59-77.

LIST OF MAIN SYMBOLS

a : Half contact ellipse length in y direction	P : Hertzian local pressure
a_1, a_2 : y rolling line location	P_H : Maximum Hertzian Pressure
b: Half ellipse length in x direction	Q : Contact load
D : Ball diameter	$R_{i,o}$: Radius to initial contact point
d_m : pitch diameter	R_a : Hertzian contact radius
dT : Torque due to one ball	$R_{x,y}$: Equivalent radius in x and y direction
dF^S : Friction force in a given contact ellipse slice	u : entrainment rolling speed = $\omega_r \cdot D/2$
$e : \frac{F^S}{\mu \cdot Q} \quad E : \frac{2 \cdot R_a}{a} \cdot \tan \gamma$	x : Direction of entrainment rolling speed
E' : Equivalent Young's modulus	X : x / b
F_a, F_r : Axial and radial force on bearing	y : Direction \perp to x
FB : Braking force on ball	Y : y/a
fc : factor used for calculating MC	z : Contact ellipse height
fp : factor used for calculating MP	Z: Number of balls
FP : Force due to the x component of the EHD pressure	α : contact angle
FR : Hydrodynamic rolling force	ϵ : Load zone parameter or value of F^S
F^S : Friction force	γ : Angle between the pure rolling contact line and ω_r .
J_a, J_r : Sjövall integrals	τ : shear stress
k : Ratio between equivalent radius R_y/R_x	μ : local friction coefficient
K : parameter defining race curvature radius: $(1+K) \cdot D/2$	α' : Pressure viscosity parameter
MB : Braking moment on ball	η_o : Dynamic viscosity at zero pressure
MC : Moment due to the contact race curvature	δ : Total normal deformation at two contact ellipse
MP : Moment due to pivoting on contact ellipse	ω_r : Rotational ball speed.
MER : Elastic rolling resistance moment	Index:
	o: Inner race
	i: Outer race